Heavy meson masses and decay constants from relativistic heavy quarks in full lattice QCD

C. McNeile,[1] C. T. H. Davies,[2,*] E. Follana,[3] K. Hornbostel,[4] and G. P. Lepage[5]
(HPQCD collaboration),[†]

[1]*Bergische Universität Wuppertal, Gaussstr. 20, D-42119 Wuppertal, Germany*
[2]*SUPA, School of Physics and Astronomy, University of Glasgow, Glasgow, G12 8QQ, UK*
[3]*Departamento de Física Teórica, Universidad de Zaragoza, E-50009 Zaragoza, Spain*
[4]*Southern Methodist University, Dallas, Texas 75275, USA*
[5]*Laboratory of Elementary-Particle Physics, Cornell University, Ithaca, New York 14853, USA*

(Dated: July 5, 2012)

We determine masses and decay constants of heavy-heavy and heavy-charm pseudoscalar mesons as a function of heavy quark mass using a fully relativistic formalism known as Highly Improved Staggered Quarks for the heavy quark. We are able to cover the region from the charm quark mass to the bottom quark mass using MILC ensembles with lattice spacing values from 0.15 fm down to 0.044 fm. We obtain $f_{B_c} = 0.427(6)$ GeV; $m_{B_c} = 6.285(10)$ GeV and $f_{\eta_b} = 0.667(6)$ GeV. Our value for f_{η_b} is within a few percent of f_Υ confirming that spin effects are surprisingly small for heavyonium decay constants. Our value for f_{B_c} is significantly lower than potential model values being used to estimate production rates at the LHC. We discuss the changing physical heavy-quark mass dependence of decay constants from heavy-heavy through heavy-charm to heavy-strange mesons. A comparison between the three different systems confirms that the B_c system behaves in some ways more like a heavy-light system than a heavy-heavy one. Finally we summarise current results on decay constants of gold-plated mesons.

arXiv:1207.0994v1 [hep-lat] 4 Jul 2012

I. INTRODUCTION

Lattice QCD calculations offer particular promise for B meson physics where a number of relatively simple weak decay processes give access to elements of the CKM matrix that are important for constraining the unitarity triangle of the Standard Model [1]. The theoretical calculation of the appropriate weak matrix elements must be done with percent accuracy for stringent constraints, making optimal use of the experimental results. This has not yet been achieved, despite the enormous success of lattice QCD over the last five years and its acceptance as a precision tool for QCD physics [2]. Work is ongoing on several different approaches. Here we continue discussion of an alternative method for B meson physics that may offer a faster route to high accuracy for some quantities than other methods currently in use. Following work on accurate b and c quark masses [3] and heavy-strange decay constants [4], we show results for masses and decay constants of B_c and η_b mesons and map out their heavy-quark mass dependence. As well as showing that high accuracy can be achieved, these results provide an interesting comparison of how heavy-charm mesons sit between heavy-heavy and heavy-light.

The calculations use a discretisation of the quark Lagrangian onto the lattice known as the Highly Improved Staggered Quark (HISQ) action [5]. This has the advantages of being numerically very fast along with having small discretisation errors and enough chiral symmetry (a PCAC relation) that the weak current that causes charged pseudoscalar mesons to decay leptonically is absolutely normalised. This action readily gives π and K meson decay constants with errors below 1% on gluon field configurations that include the full effect of u, d and s quarks in the sea [6, 7]. Results from multiple values of the lattice spacing and multiple sea u/d quark masses allow extrapolation to the real world with physical u/d quark masses at zero lattice spacing.

The HISQ action gives similarly accurate results for mesons containing c quarks [6], significantly improving on previous methods that use a nonrelativistic effective theory such as the Fermilab action [8] or NRQCD [9]. The key advantages are clear: the HISQ action has no errors from missing higher order terms in the effective theory or from the renormalisation of the decay constant [1]. The price to be paid is that of the discretisation errors. These errors are much larger for c quarks than for u/d and s, since their size is now set by $m_c a$ rather than $\Lambda_{QCD} a$. They can be well controlled, however, using the HISQ action on gluon configurations with a wide range of lattice spacing values down to 0.045 fm where $m_c a = 0.2$ [10]. Discretisation errors are in fact the only issue for the D_s meson, for which particularly accurate results can be obtained. This meson has no valence light quarks and the dependence of both its mass and decay constant on the u/d quark masses is seen to be very small [10], meaning that uncertainties from the chiral extrapolation are not significant.

It is less clear what to do for b quarks because they are so much heavier. To achieve $m_b a < 1$ we need a lattice spacing, $a < 0.04$fm. Using NRQCD or the Fermilab formalism we can readily handle b quarks on much coarser lattices, with $a \approx 0.1$ fm, but must then take a substan-

*c.davies@physics.gla.ac.uk
†URL: http://www.physics.gla.ac.uk/HPQCD

tial error (currently 4% for NRQCD [11]) from matching the weak annihilation current to full QCD perturbatively. Work is underway to reduce this error [12]. It should also be emphasised that this matching error is not present in ratios of decay constants, for example f_{B_s}/f_B which is known to 2% from NRQCD [11].

Here we show what accuracy is possible using the HISQ action for b quarks. We use quark masses heavier than that of the c quark and map out the heavy quark mass dependence of both masses and decay constants for a variety of different pseudoscalar mesons. By using experience from the D_s [10] and concentrating on mesons that do not contain valence light quarks we do not have to worry significantly about the extrapolation to the physical u/d quark mass limit. The key issue is that of discretisation errors, as for f_{D_s}, and we therefore work with the same large range of lattice spacing values from 0.15fm to 0.044fm, so that we can account fully for the a dependence. It is important to separate discretisation effects from physical dependence on the heavy quark mass since we do also have to extrapolate to the physical b mass from the quark masses that we are able to reach on these lattices. We are only able to obtain results directly at close to the physical b mass on the finest, 0.044fm lattice.

We have already demonstrated how well this method works in determining the decay constant of the B_s meson [4], one of the key quantities of interest for CKM studies. Mapping out the B_s decay constant as a function of heavy quark mass showed that the decay constant peaks around the D_s and then falls slowly. We found that $f_{B_s}/f_{D_s} = 0.906(14)$, the first significant demonstration that this ratio is less than 1.

Here we extend this work to map out results for the decay constants of the η_b and B_c mesons, along with the B_c meson mass. The B_c meson mass is known experimentally but its leptonic decay rate has not yet been measured and so we provide the first prediction of that in full lattice QCD. The masses and decay constants also reveal information about the nature of these mesons that can provide useful input to model calculations. For example, does the B_c meson look more like a heavy-heavy meson or a heavy-light meson? It is important to emphasise that both the results determined at the b quark mass and the dependence on the heavy quark mass (and on any light quark masses) have physical meaning: the former can be tested against experiment but the latter can provide stringent tests of models and comparison between lattice QCD calculations.

The layout of the paper is as follows: section II describes the lattice calculation and then section III gives results for heavy-heavy and heavy-charm mesons in turn. We compare the B_c meson mass to experiment and predict its decay constant as well as comparing the behaviour of heavy-charm mesons to that of heavyonium and heavy-strange mesons. Section V gives our conclusions, looking forward to what will be possible for b quark physics on even finer lattices in future.

Set	r_1/a	$au_0m_l^{asq}$	$au_0m_s^{asq}$	L/a	T/a	$N_{conf} \times N_t$
1	2.152(5)	0.0097	0.0484	16	48	631×2
2	2.618(3)	0.01	0.05	20	64	595×2
3	3.699(3)	0.0062	0.031	28	96	566×4
4	5.296(7)	0.0036	0.018	48	144	201×2
5	7.115(20)	0.0028	0.014	64	192	208×2

TABLE I: Ensembles (sets) of MILC configurations used for this analysis. The sea asqtad quark masses m_l^{asq} ($l = u/d$) and m_s^{asq} are given in the MILC convention where u_0 is the plaquette tadpole parameter. The lattice spacing values in units of r_1 after 'smoothing' are given in the second column [13]. Set 1 is 'very coarse'; set 2, 'coarse'; set 3, 'fine'; set 4 'superfine' and set 5 'ultrafine'. The size of the lattices is given by $L^3 \times T$. The final column gives the number of configurations used and the number of time sources for propagators per configuration.

II. LATTICE CALCULATION

We use ensembles of lattice gluon configurations at 5 different, widely separated, values of the lattice spacing, provided by the MILC collaboration. The configurations include the effect of u, d and s quarks in the sea with the improved staggered (asqtad) formalism. Table I lists the parameters of the ensembles. The u and d masses are taken to be the same, and the ensembles have $m_{u/d}/m_s$ approximately 0.2. As discussed in section I, we expect sea quark mass effects to be small for the gold-plated mesons with no valence light quarks that we study here.

The lattice spacing is determined on an ensemble-by-ensemble basis using a parameter r_1 that comes from fits to the static quark potential calculated on the lattice [13]. This parameter can be determined with very small statistical/fitting errors. However, its physical value is not accessible to experiment and so must be determined using other quantities, calculated on the lattice, that are. We have determined $r_1 = 0.3133(23)$ fm using four different quantities ranging from the (2S-1S) splitting in the Υ system to the decay constant of the η_s (fixing f_K and f_π from experiment) [14]. Using our value for r_1 and the MILC values for r_1/a given in Table I we can determine a in fm on each ensemble or, equivalently, a^{-1} in GeV needed to convert lattice masses to physical units. It is important to note that the relative values of a (from r_1/a) are determined more accurately than the absolute values of a (from r_1). Our fits account for this to give two separate errors in our error budgets.

Table I lists the number of configurations used from each ensemble and the number of time sources for the valence HISQ propagators per configuration. To increase statistics further we use a 'random wall' source for the quark propagators from a given time source. When quark propagators are combined this effectively increases the number of meson correlators sampled and reduces the statistical noise by a large factor for the case of pseudoscalar mesons. We also take a random starting point for our time sources for the very coarse, coarse and fine

ensembles.

We use many different masses for the HISQ valence quarks varying from masses close to that of the s quark to much heavier values for c quarks and for quarks with masses between c and b. On all sets the largest valence quark mass in lattice units that we use is $m_h a = 0.85$. These propagators are combined to make goldstone pseudoscalar meson correlators at zero momentum with all possible combinations of valence quark masses. We separate them into 'heavy-heavy' correlators when both masses are the same and are close to charm or heavier; 'heavy-charm' when one mass is close to charm and the other is heavier and 'heavy-strange' when one mass is close to strange and the other is close to charm or heavier.

The meson correlation function is averaged over time sources on a single configuration so that any correlations between the time sources are removed. Autocorrelations between results on successive configurations in an ensemble were visible by binning only on the finest lattices. We therefore bin the correlators on superfine and ultrafine lattices by a factor of two.

The meson correlators are fit as a function of the time separation between source and sink, t, to the form:

$$\overline{C}(t) = \sum_i a_i (e^{-M_i t} + e^{-M_i (T-t)}) \tag{1}$$

for the case of equal mass quark and antiquark. $i = 1$ is the ground state and larger i values denote radial or other excitations with the same J^{PC} quantum numbers. T is the time extent of the lattice. For the unequal mass case there are additional 'oscillating' terms coming from opposite parity states, denoted i_p:

$$\overline{C}(t) = \sum_{i,i_p} a_i e^{-M_i t} + (-1)^t a_{i_p} e^{-M_{i_p} t} + (t \to T - t) \tag{2}$$

To fit we use a number of exponentials i, and where appropriate i_p, in the range 2–6, loosely constraining the higher order exponentials by the use of Bayesian priors [15]. As the number of exponentials increases, we see the χ^2 value fall below 1 and the results for the fitted values and their errors for the parameters for the ground state $i = 1$ stabilise. This allows us to determine the ground state parameters a_1 and M_1 as accurately as possible whilst allowing the full systematic error from the presence of higher excitations in the correlation function. We take the fit parameters to be the logarithm of the ground state masses M_1 and M_{1_p} and the logarithms of the differences in mass between successive radial excitations (which are then forced to be positive). The Bayesian prior value for M_1 is obtained from a simple 'effective mass' in the correlator and the prior width on the value is taken as a factor of 1.5. The prior value for the mass splitting between higher excitations is taken as roughly 600 MeV with a width of 300 MeV. Where oscillating states appear in the fit, the prior value for M_{1_p} is taken as roughly 600 MeV above M_1 with a prior width of 300 MeV and the splitting between higher oscillating excitations is taken to be the same as for the non-oscillating states. The amplitudes a_i and a_{i_p} are given prior widths of 1.0. We apply a cut on the range of eigenvalues from the correlation matrix that are used in the fit of 10^{-3} or 10^{-4}. We also cut out very small t values from our fit, typically below 3 or 4, to reduce the effect of higher excitations.

The amplitude, a_1, from the fits in equations (1) and (2) is directly related to the matrix element for the local pseudoscalar operator to create or destroy the ground-state pseudoscalar meson from the vacuum. Using the PCAC relation this can be related to the matrix element for the temporal axial current and thence to the decay constant. The PCAC relation guarantees that no renormalisation of the decay constant is needed. We have:

$$f_P = (m_a + m_b)\sqrt{\frac{2a_1}{M_1^3}}. \tag{3}$$

for meson P. Here m_a and m_b are the quark masses used in the lattice QCD calculation.

f_P is clearly a measure of the internal structure of a meson and in turn is related, for charged pseudoscalars such as the π, K, D, D_s, B and B_c mesons, to the experimentally measurable leptonic branching fraction via a W boson:

$$\mathcal{B}(P \to l\nu_l(\gamma)) = \frac{G_F^2 |V_{ab}|^2 \tau_P}{8\pi} f_P^2 m_l^2 m_P \left(1 - \frac{m_l^2}{m_P^2}\right)^2, \tag{4}$$

up to calculable electromagnetic corrections. V_{ab} is the appropriate CKM element for quark content $a\bar{b}$. τ_P is the pseudoscalar meson lifetime. For neutral mesons there is no possibility to annihilate to a single particle via the temporal axial current. However, in the Standard Model the B_s and B are expected to annihilate to $\mu^+\mu^-$ with a rate that is proportional to $f_P^2 |V_{tb}^* V_{tq}|^2$ via 4-fermion operators in the effective weak Hamiltonian [16]. For the heavy-heavy pseudoscalar, the decay rate to two photons is related to its decay constant but only at leading order in a nonrelativistic expansion. In section III we compare the pseudoscalar decay constant to that of its associated vector meson, determined directly from its decay to leptons.

The results for masses and decay constants from fits in eqs. (1) and (2) and using eq. (3) are in units of the lattice spacing, and given in this form in the tables of section III. To convert to physical units, as discussed earlier, we determine the lattice spacing using the parameter r_1.

We then fit the results in physical units as a function of heavy quark mass to determine the heavy quark mass dependence and the physical value at the b quark mass. Because the bare heavy quark mass used in the lattice action runs with lattice spacing we need a proxy for it that is a physical quantity, such as a meson mass. In [4] we used the heavy-strange pseudoscalar mass since we were focussing on heavy-strange mesons. Here we choose

	electromagnetism	c-in-sea	annihiln to g
M_{η_b}	-1.6(8)	-5(3)	-2.4(2.4)
M_{η_c}	-2.6(1.3)	-0.4(2)	-2.4(1.2)
M_{B_c}	+2(1)	-1(1)	-
M_{B_s}	-0.1(1)	-	-
M_{D_s}	+1.3(7)	-	-

TABLE II: Estimates of shifts in MeV to be applied to the masses determined in lattice QCD to allow for missing electromagnetism, c quarks in the sea and annihilation to gluons for the η_b and η_c mesons [10, 18]. The electromagnetic shift is estimated from a potential model for η_b, η_c and B_c and from a comparison of charged and neutral meson masses for B_s and D_s. The c-in-sea and gluon annihilation shifts are estimated from perturbation theory. The errors on the shifts are given in brackets. Note that for the η_S there are no shifts because the mass is fixed in lattice QCD [14].

	form of f_0	b	A	c_{0000}	c_{ijkl}
f_{η_h}	$A(M/M_0)^b$	0 ± 1	0 ± 2	1	0 ± 4.5
$\Delta_{H_s,hh}$	$A(M/M_0)^b$	1	1	0 ± 2	0 ± 1.5
f_{H_s}	$A(\frac{\alpha_V(M)}{\alpha_V(M_{\eta_c})})^{-2/9}(\frac{M}{M_0})^b$	-0.5	0 ± 2	1	0 ± 1.5
$\Delta_{H_c,hh}$	$A((M-M_{\eta_c})/M_0)^b$	1	1	0 ± 2	0 ± 1.5
f_{H_c}	$A(\frac{\alpha_V(M)}{\alpha_V(M_{\eta_c})})^{-2/9}(\frac{M}{M_0})^b$	-0.5	0 ± 2	1	0 ± 3
$\Delta_{H_c,hs}$	$A(M/M_0)^b$	0	1	0 ± 2	0 ± 1.5

TABLE III: The functional form for $f_0(M)$, the leading power dependence on the heavy quark mass, used in fitting the different quantities described in section III using equation (5). The third and fourth columns give the prior values and widths for the parameters A and b. In most cases b was fixed and then a single number is given. Likewise the sixth column gives the prior value and width for the c_{ijkl} where the sum was normalised so that c_{0000} was set equal to 1.

the mass of the heavy-heavy pseudoscalar meson, η_h, to provide the same x-axis for all of our plots showing dependence on the heavy quark mass. The positions of c and b on these plots are then determined by the values of the η_c and η_b masses.

The experimental results for the η_b and η_c meson masses are 9.391(3) GeV and 2.981(1) GeV respectively [17]. Our lattice QCD calculation, however, is missing some ingredients from the real world which means that we must adjust the experimental values we use in our calibration. The key missing ingredients are electromagnetism, c quarks in the sea and the possibility for the η_b and η_c mesons to annihilate to gluons, which we do not allow for in determining our η_c and η_b correlators. These effects all act in the same direction, that of lowering the meson mass in the real world compared to that in our lattice QCD world. We estimate the total shift from these effects for the η_c to be -5.4(2.7) MeV and for the η_b, as -9(6) MeV [18]. The appropriate 'experimental' masses for the η_c and η_b for our calculations are then 2.986(3) GeV and 9.400(7) GeV.

Since we need to allow for the three ingredients missing from our lattice QCD calculation when we determine meson masses in section III, we give in Table II a summary of our estimates of these effects [10, 18]. These estimates will be used to shift the lattice QCD results for comparison to experiment. Effects on decay constants are much smaller and we do not apply shifts in that case but simply include an additional uncertainty in the error budget.

For consistency we fit a similar functional form to all quantities. This form must take account of physical heavy quark mass-dependence; discretisation errors and, for heavy-charm and heavy-strange mesons, mistuning of c and s quark masses. We use the standard constrained fitting techniques that we earlier applied to the correlators [15]. For the dependence on heavy quark mass and lattice spacing for each set of results $f(M,a)$, we use

$$f(M,a) = f_0(M) \times \sum_{i=0}^{7}\sum_{j,k=0}^{3}\sum_{l=0}^{1} c_{ijkl}\left(\frac{M_0}{M}\right)^i (\frac{am_1}{\pi})^{2j}(\frac{am_2}{\pi})^{2k}(\frac{a\Lambda}{\pi})^{2l} + \delta f_s + \delta f_c \quad (5)$$

The quantity that we use for the heavy quark mass, M, is given by $M = M_{\eta_h}$. f_0 is a function giving the 'leading power' behaviour expected for each quantity. This is either derived from HQET or potential model expectations and takes the general form $A(M/M_0)^b$. For the decay constants f_{H_c} and f_{H_s} we multiply this by the ratio of α_s values at the b and the c raised to the power of $-2/\beta_0$ = -2/9 for $n_f = 3$. This is the expected prefactor from resumming leading logarithms in HQET [19]. For α_s we take α_V from lattice QCD [3, 20]. We take M_0 to have the value 2 GeV so that the factor M_0/M is approximately $1\text{GeV}/m_b$. We tabulate the different forms for f_0 in Table III along with the prior values taken for A and b. b is allowed to float for the fit to f_{η_h}. In other cases it is fixed to the expected value but we have checked that allowing it to float returns the expected value within errors. We take the same prior for A of 0 ± 2 in all cases.

The sum to the right of the leading term includes higher order corrections to the physical mass-dependence. These take the form of powers of M_0/M, again using $M_0 = 2\,\text{GeV}$. We allow for 8 terms in the sum so that there is enough leeway to describe (by Taylor's theorem) any physically reasonable functional form in the fixed mass range from c to b. For the heavy-charm case we in fact fit from $M = 4\,\text{GeV}$ upwards so that the functional form is that appropriate to the unequal valence mass case.

The other terms in the sum of eq. (5) allow for systematic errors resulting from sensitivity to the lattice spacing. Such discretisation errors depend on the lattice momentum cut-off, π/a, but can have a scale set by the different masses involved in the quantity under study. We allow for discretisation errors appearing with a scale of

m_1 and m_2, where m_1 and m_2 are the two quark masses in the meson (they will be the same in heavyonium). To be conservative we allow in addition further discretisation errors with a scale of $\Lambda_{\rm QCD}$ where we take $\Lambda_{\rm QCD} = 0.5$ GeV. The powers of lattice spacing that appear in the terms must be even since discretisation errors only appear as even powers for staggered quarks. For the decay constants the c_{ijkl} are normalised so that $c_{0000} = 1$. For the mass differences the fits are normalised so that A is 1 and c_{0000} floats. This is simply so that the fit can allow for significant discretisation errors when the physical mass difference is very small (particularly for the case of the B_c to be discussed in section III C). The prior values for the other c_{ijkl} are taken to be the same for all i, j, k and l but vary depending on the size of discretisation errors for the quantity being fit. They are larger for heavyonium than for heavy-strange quantities, for example. The values used are tabulated in Table III.

The mistuning of the strange and charm quark masses, where relevant, can be handled very simply because our tuning of these masses is in fact very good. We simply include an additional additive factor in the fit of

$$\delta f_s = (c_s + \frac{d_s}{M} + e_s\left[\left(\frac{am_1}{\pi}\right)^2 + \left(\frac{am_2}{\pi}\right)^2\right]) \times (m^2_{\eta_s,\rm latt} - m^2_{\eta_s,\rm contnm}) \quad (6)$$

for heavy-strange mesons and

$$\delta f_c = (c_c + \frac{d_c}{M} + e_c\left[\left(\frac{am_1}{\pi}\right)^2 + \left(\frac{am_2}{\pi}\right)^2\right]) \times (m_{\eta_c,\rm latt} - m_{\eta_c,\rm contnm}) \quad (7)$$

for heavy-charm mesons. The forms above allow for linear quark mass dependence away from the tuned point. We do not need to include higher order terms because we are so close to the tuned point but we do allow for an M-dependent slope with discretisation errors (although in most cases neither of these additions makes any difference).

To tune the strange quark mass we use the η_s, an unphysical $s\bar{s}$ pseudoscalar meson whose valence quarks are not allowed to annihilate. Lattice QCD simulations show that its mass $m_{\eta_s,\rm contnm} = 0.6858(40)$GeV [14] when the strange quark mass is tuned (from the K meson). Being a light pseudoscalar meson, the square of its mass is proportional to the quark mass. To tune the c quark mass we use the η_c meson, as discussed earlier. The η_c meson is far from the light quark limit and so the meson mass is simply proportional to the quark mass. c_s and c_c are dimensionful coefficients that represent physical light quark mass dependence and can be compared between lattice QCD calculations and with models.

We do not include correlations between the results for different M on a given ensemble. We have not measured these correlations and the empirical Bayes criterion suggests that they are small. If we include a correlation matrix by hand for the results it makes very little difference, a fraction of a standard deviation, to the final results.

Set	$m_h a$	ϵ	$M_{\eta_h} a$	$f_{\eta_h} a$
1	0.66	-0.244	1.92020(16)	0.3044(4)
	0.81	-0.335	2.19381(16)	0.3491(5)
	0.825	-0.344	2.22013(15)	0.3539(5)
	0.85	-0.359	2.26352(15)	0.3622(5)
2	0.44	-0.12	1.42402(13)	0.21786(21)
	0.63	-0.226	1.80849(11)	0.25998(20)
	0.66	-0.244	1.86666(10)	0.26721(20)
	0.72	-0.28	1.98109(10)	0.28228(22)
	0.753	-0.3	2.04293(10)	0.29114(24)
	0.85	-0.36	2.21935(10)	0.31900(27)
3	0.3	-0.06	1.03141(8)	0.15205(11)
	0.413	-0.107	1.28057(7)	0.17217(11)
	0.43	-0.115	1.31691(7)	0.17508(11)
	0.44	-0.12	1.33816(7)	0.17678(11)
	0.45	-0.125	1.35934(7)	0.17850(11)
	0.7	-0.27	1.86536(5)	0.22339(12)
	0.85	-0.36	2.14981(5)	0.25658(12)
4	0.273	-0.0487	0.89935(10)	0.11864(24)
	0.28	-0.051	0.91543(8)	0.11986(21)
	0.564	-0.187	1.52542(6)	0.16004(16)
	0.705	-0.271	1.80845(6)	0.18071(16)
	0.76	-0.305	1.91567(6)	0.18962(17)
	0.85	-0.359	2.08753(6)	0.20576(16)
5	0.193	-0.0247	0.66628(13)	0.0882(3)
	0.195	-0.02525	0.67117(6)	0.08846(11)
	0.4	-0.101	1.13276(7)	0.1149(4)
	0.5	-0.151	1.34477(8)	0.1260(5)
	0.7	-0.268	1.75189(7)	0.1498(5)
	0.85	-0.359	2.04296(7)	0.1708(6)

TABLE IV: Results for the masses and decay constants in lattice units of the goldstone pseudoscalars made from valence HISQ heavy quarks on the different MILC ensembles, enumerated in Table I. Columns 2 and 3 give the corresponding bare heavy quark mass and the ϵ parameter, calculated at tree-level in $m_h a$ [10]. This corresponds to a coefficient for the Naik 3-link discretisation correction of $1 + \epsilon$. Meson masses from fitting these correlators using a simpler fitting form are given in [3]. Results given here are in agreement but somewhat more accurate. The results for heavy quark masses close to charm are also given in [10].

We also do not include effects from sea quark mass-dependence but, based on earlier work [10], we are able to estimate an uncertainty for that in our final results.

III. RESULTS

A. f_{η_b}

The correlators for pseudoscalar heavyonium mesons have very little noise and we can readily obtain ground-state masses with statistical errors in the fourth or fifth decimal place and ground-state decay constants with errors of 0.1%. Our results on each ensemble are given in Table IV.

Results for f_{η_h} are plotted against M_{η_h} in Figure 1. Discretisation errors are apparent in this plot and lead

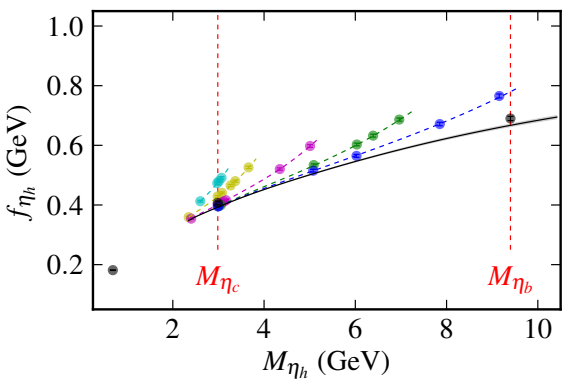

FIG. 1: Results for the pseudoscalar heavyonium decay constant plotted as a function of the pseudoscalar heavyonium mass. Results for very coarse, coarse, fine, superfine and ultrafine lattices appear from left to right. The colored dashed lines give the fitted function for that lattice spacing. The black line with grey error band gives the physical curve derived from our fit. The black circles with error bars at M_{η_c} and M_{η_b} are the values for the heavyonium vector decay constant at these physical points derived from the experimental leptonic widths for the J/ψ and Υ. The left-most black circle corresponds to the fictitious pseudoscalar η_s particle whose decay constant was determined in [14].

to results at each value of the lattice spacing deviating substantially from the physical curve as the quark mass is increased. We fit the results to a physical curve allowing for discretisation errors as a function of the mass, as described in section II and using the priors from Table III. The power, b, in eq. (5) is allowed to float in the fit.

The obvious approach from which to gain some physical insight in this case is that of the nonrelativistic potential model. In its simplest form this involves solving Schrödinger's equation for the wavefunction of a two-particle system with reduced mass μ ($= m_b/2$ for two b quarks) in a potential $V(r)$ which is a function of the radial separation, r. At short distances we expect a Coulomb-like potential from QCD, and at large distances a string-like linear potential. However, other phenomenological forms that interpolate between these two at intermediate distances also work well at reproducing the bound-state spectrum, see for example [21]. The wavefunction is useful for a first approximation in calculations of transition rates. In this sense, the wavefunction at the origin, $\psi(0)$, can be related to the decay constant by $\psi(0) = f_{\eta_h}\sqrt{M_{\eta_h}/12}$. However, $\psi(0)$ must be renormalised before it can be related to a physical matrix element and some of the radiative corrections are very substantial [21]. In addition values of $\psi(0)$ vary widely with different forms for the potential that reproduce the same bound state spectrum because the spectrum itself provides little constraint on the potential at short distances [22]. Here we will make comparisons of our lattice QCD results to those from potential models but it is important to realise that the lattice QCD results for decay constants represent well-defined matrix elements in QCD and not model calculations.

For a potential model with potential r^N power counting arguments yield $\psi(0) \propto \mu^{3/(4+2N)}$ (see, for example, [23]). Then we would expect our fit for f_{η_h} to need $b = 1$ for $N = -1$ but $b = 0$ for $N = 1$, the two extremes of the QCD heavy quark potential. Simply from comparing values at c and b we might infer $b \approx 0.5$. In fact our fit gives the result $b = -0.08(10)$ but with significant power corrections in $1/M$, so that a simple power in M does not describe the results using our parameterisation. The physical curve that we extract of dependence on the heavyonium meson mass is shown as the grey band in Figure 1.

The fit has χ^2 of 1.2 for 29 degrees of freedom and allows us to extract results for c and b quarks. The result for f_{η_c} agrees within 1σ with our earlier result of 0.3947(22) GeV [10] where we fit results at c only but included additional ensembles at different values of the sea u/d quark masses. Results for b quarks give:

$$\begin{aligned} f_{\eta_b} &= 0.667(6)(2)\text{GeV} \\ f_{\eta_b}/f_{\eta_c} &= 1.698(13)(5). \end{aligned} \tag{8}$$

The first error comes from the fit and the second from additional systematic errors from effects not included in our lattice QCD calculation, i.e. electromagnetism, c quarks in the sea and (since we have not extrapolated to physical u/d sea quark masses here) sea quark mass effects. Both errors are split into their component parts in the error budget of Table V. We estimated the effects of electromagnetism on f_{η_c} from a potential model in [10]. We take the same 0.4% error for f_{η_b} since it is a more tightly bound particle but with smaller electromagnetic charges. There is then some cancellation of the effect in the ratio f_{η_b}/f_{η_c}. The effects of c quarks in the sea were shown to be similar to that of the hyperfine potential in [10] and the effect on f_{η_h} can then be estimated from the difference between f_{η_h} and its associated vector particle. This is very small as we show below. We therefore expect that missing c in the sea has a negligible effect on f_{η_c} and we estimate 0.2% on f_{η_b} where it is magnified by $(m_b/m_c)^2$. Sea quark mass effects on f_{η_c} were shown to be very small in [10], at the same level as the statistical errors of 0.1%. For f_{η_b} we expect even smaller effects because it is a smaller particle. We take a 0.1% error nevertheless, but allow for some cancellation in the ratio of f_{η_b}/f_{η_c}.

The two rightmost black points (at M_{η_b} and M_{η_c}) in Fig. 1 give the experimental values for the decay constants of the corresponding vector heavyonium mesons, J/ψ and Υ, for comparison to the results calculated here in lattice QCD for the η_c and η_b. The decay constant for a vector meson can be defined by:

$$\sum_i < 0|\overline{\psi}\gamma_i\psi|V_i > /3 = f_V m_V. \tag{9}$$

Error	f_{η_b}	f_{η_b}/f_{η_c}
statistics	0.6	0.6
M extrapoln	0.2	0.1
a^2 extrapoln	0.5	0.4
r_1	0.4	0.1
r_1/a	0.5	0.3
M_{η_c}	0.00	0.05
sea quark mass effects	0.1	0.05
electromagnetism	0.4	0.2
c in the sea	0.2	0.2
Total (%)	1.0	0.9

TABLE V: Full error budget for f_{η_b} and the ratio f_{η_b}/f_{η_c} in %. See text for a fuller description of each error. The total error is obtained by adding the individual errors in quadrature.

It has the advantage here that it can be extracted very accurately from experiment because vector heavyonium mesons can annihilate, through the vector currrent, to a photon, seen as two leptons in the final state. The relationship between the leptonic decay width and the decay constant is:

$$\Gamma(V_h \to e^+e^-) = \frac{4\pi}{3}\alpha_{QED}^2 e_h^2 \frac{f_V^2}{m_V} \qquad (10)$$

where e_h is the electric charge of the heavy quark in units of e. The experimental results [17] give $f_{J/\psi} = 407(5)$ MeV and $f_\Upsilon = 689(5)$ GeV, remembering that the electromagnetic coupling constant runs with scale and using $1/\alpha_{QED}(m_c) = 134$ and $1/\alpha_{QED}(m_b) = 132$[24]. Thus 1% accurate results for this decay constant are available from experiment, and can be used to test lattice QCD. Lattice QCD calculations of the Υ decay constant can be done [25] but they are not yet as accurate as the results we give here for the η_b.

The surprising result that we find on comparing the vector decay constant from experiment to the pseudoscalar decay constant from lattice QCD is how close they are. In the nonrelativistic limit, where spin effects disappear, the vector and pseudoscalar become the same particle. Away from this point, however, there can be substantial relativistic corrections, particularly for charmonium. Instead we find that the pseudoscalar decay constant is 3% lower than the vector in both cases with an error of 1-2%.

Unfortunately this cannot be directly tested through decay modes of the η_c or η_b. The decay rate to two photons is indirectly related to the decay constant as the leading term in a nonrelativistic approximation:

$$\Gamma(\eta_h \to \gamma\gamma) = \frac{12\pi e_h^4 \alpha_{QED}^2 |\psi(0)|^2}{m_h^2}. \qquad (11)$$

This formula has radiative and relativistic corrections at the next order. The decay width is not known for the η_b and only very poorly known for the η_c, with the Particle Data Group estimate given as 7.2(2.1) keV [17]. Substituting this into eq. (11) and taking $m_c = M_{\eta_c}/2$, justifiable at this order, gives $f_{\eta_c} = 0.4(1)$ GeV, where only the large error from experiment is shown. This is consistent with our value but much less accurate so does not provide a useful test.

As discussed earlier, a direct comparison of lattice QCD results for f_{η_h} and potential model values for $\psi(0)$ is not particularly useful. Values for $\psi(0)$ for the ground state in bottomonium vary by a factor of 1.5 for different forms for the potential in [22]. This variation is reduced somewhat, and radiative corrections cancel, if we compare the ratio of values at b and c. Here the lattice QCD result above of 1.698(14) favours the strong variation of $\psi(0)$ with quark mass seen in the Cornell potential. For this potential [22] gives a ratio $\psi_b(0)/\psi_c(0)$ of 3.1, yielding a decay constant ratio of 1.8.

Figure 1 also includes as the leftmost black point a value for the decay constant of the η_s as determined from lattice QCD [14]. Although our fit becomes unstable below M of 2 GeV, it is interesting to see that f_{η_s} does not look out of place on this plot as the light and heavy sectors are smoothly connected together.

B. m_{B_s} and f_{B_s}

Our calculations for heavy-strange mesons were described in [4] and so we only add briefly to that discussion here. In Table VI we give our full set of results, including values at a variety of strange quark masses for completeness. In [4] we used the heavy-strange mass itself as a proxy for the heavy quark mass and obtained good agreement for the mass of the B_s with experiment and a value for f_{B_s} of 225(4) MeV.

Here, for consistency with the other calculations, we use instead M_{η_h} for the heavy quark mass and the fit form given in eq. (5). For the heavy-strange meson mass, as in [4], we fit to the mass difference:

$$\Delta_{H_s,hh} = m_{H_s} - \frac{m_{\eta_h}}{2}. \qquad (12)$$

We take account of mistuning of the strange quark mass using the factor given in eq. (6). For the decay constant fit we fix the power of the leading M-dependence, $b = -0.5$. Allowing b to float gives results for b in agreement with this value to within 20%.

Our fit to $\Delta_{H_s,hh}$a is shown in Figure 2 and gives $\chi^2 = 0.2$ for 17 degrees of freedom. The values extracted at the c and b masses agree well, within 1σ, with our earlier results [4, 10]. When account is taken of electromagnetic and other effects missing in the lattice calculation these earlier results translate into values for $m_{D_s} = 1.969(3)\,\mathrm{GeV}$ [10] and $m_{B_s} = 5.358(12)\,\mathrm{GeV}$ [4]. The increased error at the b results from increased statistical and discretisation errors for heavier quark masses as well as the extrapolation in M. Our result for m_{B_s} agrees within the 12 MeV error with that determined from full lattice QCD using a completely different

Set	$m_s a$	$M_{\eta_s} a$	$m_h a$	$M_{H_s} a$	$f_{H_s} a$
1	0.061	0.50490(36)	0.66	1.3108(6)	0.1913(7)
			0.81	1.4665(8)	0.1970(10)
	0.066	0.52524(36)	0.66	1.3164(5)	0.1929(7)
			0.825	1.4869(7)	0.1994(10)
2	0.0492	0.41436(23)	0.44	0.9850(4)	0.1500(5)
			0.63	1.2007(5)	0.1559(7)
			0.85	1.4289(8)	0.1613(10)
	0.0546	0.43654(24)	0.44	0.9915(4)	0.1516(5)
			0.66	1.2391(5)	0.1586(6)
			0.85	1.4348(7)	0.1634(9)
3	0.0337	0.29413(12)	0.3	0.70845(17)	0.1054(2)
			0.413	0.84721(23)	0.1084(2)
			0.7	1.1660(4)	0.1112(5)
			0.85	1.3190(5)	0.1123(6)
	0.0358	0.30332(12)	0.3	0.71119(16)	0.1061(2)
			0.43	0.86982(23)	0.1094(2)
			0.44	0.88152(23)	0.1096(3)
			0.7	1.1684(4)	0.1121(4)
			0.85	1.3214(5)	0.1131(6)
	0.0366	0.30675(12)	0.3	0.71223(16)	0.1063(2)
			0.43	0.87079(22)	0.1097(2)
			0.44	0.88249(23)	0.1099(3)
			0.7	1.1694(4)	0.1124(4)
			0.85	1.3223(5)	0.1135(6)
4	0.0228	0.20621(19)	0.273	0.59350(24)	0.0750(3)
			0.564	0.9313(5)	0.0754(6)
			0.705	1.0811(8)	0.0747(8)
			0.85	1.2279(10)	0.0742(10)
5	0.0161	0.15278(28)	0.193	0.43942(33)	0.0553(4)
			0.5	0.8027(10)	0.0541(12)
			0.7	1.0152(18)	0.0513(22)
			0.85	1.1657(24)	0.0495(30)
	0.0165	0.15484(14)	0.195	0.44270(28)	0.0555(3)
			0.5	0.8038(8)	0.0546(11)
			0.7	1.0169(12)	0.0526(16)
			0.85	1.1684(16)	0.0517(21)

TABLE VI: Results for the masses and decay constants in lattice units of the goldstone pseudoscalars made from valence HISQ heavy quarks with valence HISQ strange quarks on the different MILC ensembles, enumerated in Table I. Column 2 gives the s mass in lattice units, with several values on some ensembles around the correctly tuned value. Column 3 gives the corresponding mass for the goldstone pseudoscalar made from the s quarks, which is used for tuning. Column 4 gives the heavy quark mass. The corresponding values of the Naik coefficient are given in Table IV. Many of these results were given earlier in [4, 10].

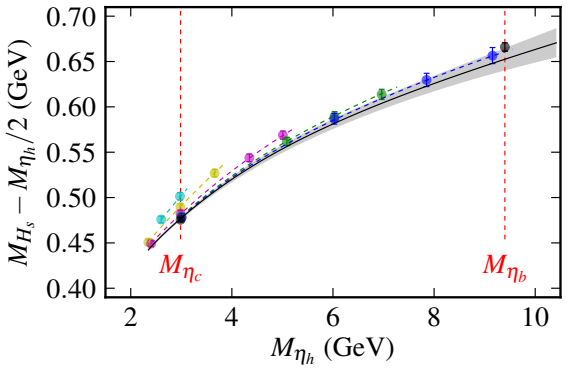

FIG. 2: Results for the difference, $\Delta_{H_s,hh}$ between the heavy-strange pseudoscalar meson mass and one half of the pseudoscalar heavyonium mass. Results for very coarse, coarse, fine, superfine and ultrafine lattices appear from left to right. The lattice QCD results have been adjusted for slight mistuning of the s quark mass. The colored dashed lines give the fitted function for that lattice spacing. The black dashed line with grey error band gives the physical curve derived from our fit. The black circles with error bars at M_{η_c} and M_{η_b} are the experimental values adjusted for the effects from electromagnetism, η_b/η_c annihilation and c quarks in the sea, none of which is included in the lattice QCD calculation.

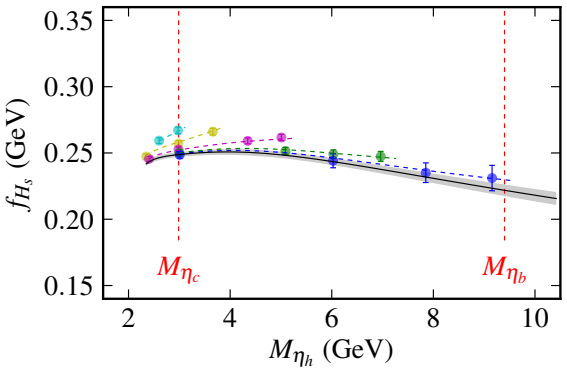

FIG. 3: Results for the pseudoscalar heavy-strange decay constant plotted as a function of the pseudoscalar heavyonium mass. Results for very coarse, coarse, fine, superfine and ultrafine lattices appear from left to right. The lattice QCD results have been adjusted for slight mistuning of the s quark mass. The colored dashed lines give the fitted function for that lattice spacing. The black dashed line with grey error band gives the physical curve derived from our fit.

method (NRQCD) for the b quark [18] with very different systematic errors, providing a stringent test of lattice QCD. Our results also agree well with experiment [17] ($m_{D_s} = 1.968\,\text{GeV}$ and $m_{B_s} = 5.367\,\text{GeV}$) and this provides a very strong test of QCD.

The fit to the decay constant, f_{H_s}, is shown in Figure 3 and gives $\chi^2 = 0.3$ for 17 degrees of freedom. Again results at the b and c agree within 1σ with our earlier results which are: $f_{D_s} = 0.2480(25)\,\text{GeV}$ [10] and $f_{B_s} = 0.225(4)\,\text{GeV}$ [4].

Figures 2 and 3 give the physical fit curves as a function of M_{η_h}. As expected, the curves are very similar to those in [4] since to a large extent the change is simply a rescaling of the x-axis. However they provide a consistency check that the parameterisation we use here, taking a different quantity to represent the heavy quark mass, works just as well.

Set	$m_c a$	$m_h a$	$M_{H_c} a$	$f_{H_c} a$
2	0.63	0.85	2.01651(10)	0.2854(2)
3	0.413	0.7	1.57733(7)	0.1916(2)
		0.85	1.72373(6)	0.2004(1)
	0.43	0.7	1.59489(7)	0.1938(2)
		0.85	1.74105(6)	0.2030(1)
	0.44	0.7	1.60522(6)	0.1952(1)
		0.85	1.75122(6)	0.2044(1)
4	0.273	0.564	1.21799(8)	0.1329(2)
		0.705	1.36350(8)	0.1367(2)
		0.76	1.41872(8)	0.1380(2)
		0.85	1.50727(8)	0.1402(2)
	0.28	0.564	1.22562(8)	0.1338(2)
		0.705	1.37103(8)	0.1376(2)
		0.76	1.42621(9)	0.1390(2)
		0.85	1.51471(9)	0.1413(2)
5	0.195	0.4	0.90566(8)	0.0967(3)
		0.5	1.01457(9)	0.0985(4)
		0.7	1.22392(10)	0.1005(4)
		0.85	1.37366(10)	0.1018(5)

TABLE VII: Results for the masses and decay constants in lattice units of the goldstone pseudoscalars made from valence HISQ heavy quarks with valence HISQ charm quarks on the different MILC ensembles, enumerated in Table I. Set 1 is missing because $m_c a$ is already close to the highest heavy quark mass that we use. Column 2 gives the c mass in lattice units, with several values on some ensembles around the tuned c mass, and column 3 the heavy quark mass. The corresponding values of the Naik coefficient are given in Table IV.

C. m_{B_c} and f_{B_c}

Heavy-charm mesons are of interest because a family of gold-plated $b\bar{c}$ mesons exists of which only one, the pseudoscalar B_c [26, 27], has been seen. Traditionally these particles have been viewed as further examples, beyond $b\bar{b}$ and $c\bar{c}$, of a heavy-heavy system and therefore a test of our understanding of this area. $b\bar{c}$ mesons, however, have a lot in common with heavy-light systems. In fact they provide a bridge between heavy-heavy and heavy-light and so test our contol of QCD much more widely. The more accurately we can do these tests, the better they are.

Lattice QCD calculations of the B_c mass can be done very accurately. Indeed the mass of the B_c was predicted ahead of experiment with a 22 MeV error [28] using NRQCD for the b quark and the 'Fermilab' clover action for the c quark. The error was later reduced to 10 MeV by using a more highly improved action, HISQ, for the charm quark [18]. Here we use the HISQ action for both the c quark and the heavier quark up to the b mass to obtain results in a completely different heavy quark formalism. In addition we calculate the decay constant of the B_c for the first time in full lattice QCD.

To determine the B_c mass we use the mass difference to the average of the associated heavyonium states:

$$\Delta_{H_c,hh} = M_{H_c} - \frac{1}{2}(M_{\eta_c} + M_{\eta_h}). \qquad (13)$$

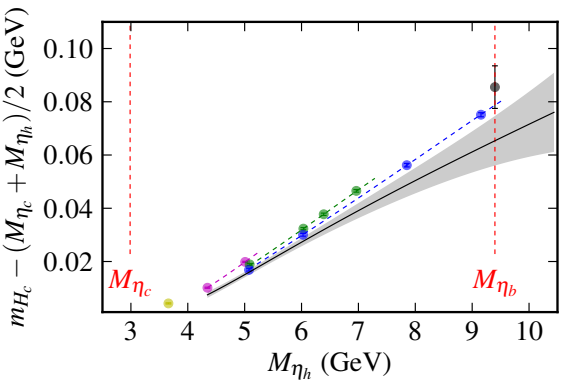

FIG. 4: Results for the mass difference between the H_c meson and the average of the associated heavyonium pseudoscalar meson masses plotted as a function of the pseudoscalar heavyonium mass. Results for coarse, fine, superfine and ultrafine lattices appear from left to right. The lattice QCD results have been adjusted for slight mistuning of the c quark mass. The colored dashed lines give the fitted function for that lattice spacing. The black line with grey error band gives the physical curve derived from our fit. The black circle with error bar at M_{η_b} gives the experimental value adjusted for the effects from electromagnetism, η_b/η_c annihilation and c quarks in the sea, none of which is included in the lattice QCD calculation.

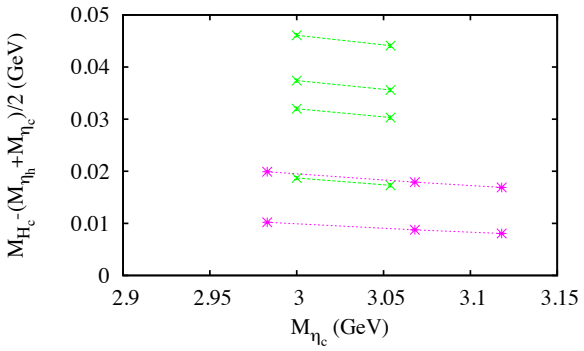

FIG. 5: Results for the mass difference between the H_c meson and the average of the associated heavyonium pseudoscalar meson masses plotted as a function of the pseudoscalar charmonium mass. Results are given for two heavy quark masses on fine lattice set 3 (pink bursts) and four heavy quark masses on superfine lattices set 4 (green crosses). Lines are drawn to guide the eye.

$\Delta_{H_c,hh}$ is a measure of the difference in binding energy between the symmetric heavyonium states made of c and h quarks and the heavyonium state made of two different mass quarks, c and h. Here we map out $\Delta_{H_c,hh}$ as a function of the heavy quark mass, and reconstruct M_{B_c} from $\Delta_{H_c,hh}$ determined at $h = b$. $\Delta_{H_c,hh}$ can be determined with high statistical accuracy because all of the states involved have very little noise. The fact that $\Delta_{H_c,hh}$ is

very small (0 for $m_h = m_c$ by definition and less than 100 MeV when $m_h = m_b$) also means that lattice errors from, for example, the uncertainty in the lattice spacing are very small. In fact, for this calculation, as discussed below, key sources of error are the uncertainties from electromagnetic, annihilation and c-in-the-sea shifts to the masses.

Table VII gives our results for the masses and decay constants of the H_c mesons calculated using quark masses that are close to that of the c quark mass on each ensemble and then all the heavier masses for h. We give results for more than one value of the c quark mass on the fine and superfine ensembles (sets 3 and 4) so that slight mis-tuning in the c quark mass can be corrected for. It is clear from the results that $\Delta_{H_c,hh}$ can be calculated with a statistical accuracy of better than 1 MeV. Errors from uncertainties in the lattice spacing are also at this level.

Figure 4 shows $\Delta_{H_c,hh}$ plotted against M_{η_h} for the results at different values of the lattice spacing. A fairly clear linear dependence is evident. $\Delta_{H_c,hh}$ would be expected to increase linearly with M_{η_h} at large M_{η_h}, in the same way as $\Delta_{H_s,hh}$, from a simple potential model argument. The binding energy of the η_h becomes increasingly negative, roughly in proportion to M_{η_h} as it increases (at least for a r^N potential with $N = -1$), whilst the binding energy of the H_c meson does not change. A corollary of this is that the dependence of $\Delta_{H_c,hh}$ on M_{η_c} (as proxy for m_c) would also then be expected to be linear with a slope of opposite sign and roughly three times the magnitude. The factor of three is because the binding energy of the η_c becomes more negative as M_{η_c} increases, with the same dependence as the η_h binding energy has on M_{η_h}. The H_c binding energy will also become more negative but have double the slope because the reduced mass of the H_c system is roughly m_c rather than $m_c/2$ for the η_c. On top of this M_{η_c} appears halved in $\Delta_{H_c,hh}$.

Interestingly this factor of -3 does seem to be approximately true in comparing Figure 5, which shows the dependence of $\Delta_{H_c,hh}$ on M_{η_c}, with Figure 4. Figure 4 gives a slope of ≈ 0.012 (over the full range) and Figure 5 gives slopes varying from -0.03 to -0.04 over a small range in M_{η_c}, as M_{η_h} increases. In our fit to $\Delta_{H_c,hh}$ we include the effect of mistuning m_c (from eq. (7)) and obtain consistent values from that.

We fit $\Delta_{H_c,hh}$ as a function of M_{η_h} (above 4 GeV) using the fit form described in section II. The leading mass dependence is taken to be $M_{\eta_h} - M_{\eta_c}$, so that $\Delta_{H_c,hh}$ vanishes when $M_{\eta_h} = M_{\eta_c}$ as it must by definition. As described in section II we include a sum of power correction terms and lattice spacing dependent terms with priors given in Table III. The fit gives χ^2 of 0.3 for 11 degrees of freedom and result:

$$\Delta_{B_c,bb} = 0.065(9)\text{GeV}. \tag{14}$$

The resulting physical curve of heavy quark mass dependence is shown in grey on Figure 4. The comparison to experiment is given by the black dot with error bar at $h = b$. This experimental result has been shifted to be the appropriate value to compare to our lattice QCD calculation as we now describe. The current world-average experimental result for $M_{B_c} - 0.5(M_{\eta_c} + M_{\eta_b})$ is 92(6) MeV [17]. There is a sizeable experimental error coming mainly from the B_c but also from the η_b. Our lattice QCD calculation is done in a world without electromagnetism or c quarks in the sea and in which the η_b and η_c do not annihilate. The absence of these effects (i.e. to compare to our lattice result) produces shifts to the masses as discussed in section II. Estimated values for the shifts are given in Table II. The net effect is to shift the experimental value of $\Delta_{B_c,hh}$ down by -8(7) MeV, where the error takes the shifts to be correlated. The 'experimental' value of $\Delta_{B_c,hh}$ to compare to our lattice result is then 84(9) MeV, marked on Figure 4. Our lattice result agrees with experiment, once these shifts are made, within 2σ.

Error	$\Delta_{B_c,bb}$	f_{B_c}	$\Delta_{B_c,bs}$
statistics	8.4	0.7	0.5
M extrapoln	3.1	0.2	0.2
a^2 extrapoln	10.9	0.7	0.4
r_1	0.7	0.6	0.3
r_1/a	1.4	0.8	0.3
M_{η_c}	0.9	0.5	0.3
sea quark mass effects	1.5	0.1	0.1
electromagnetism	3.1*	0.4	0.2*
c in the sea	5.3*	0.04	0.1*
$\eta_{b,c}$ annihiln	2.7*	-	-
Total (%)	18	1.6	0.9

TABLE VIII: Full error budget for $\Delta_{B_c,bb}$, f_{B_c} and $\Delta_{B_c,bs}$ given as a percentage of the value. See the text for a fuller description of each error. The total error is obtained by adding the individual errors in quadrature, except for the final three systematic errors (starred) for $\Delta_{B_c,bb}$ and $\Delta_{B_c,bs}$ which are correlated and so simply added together before being combined in quadrature with the others.

From $\Delta_{B_c,bb}$ we can reconstruct the B_c meson mass, now applying the shifts above to the lattice QCD calculation to obtain a result that can be compared to experiment. This gives the result

$$M_{B_c} = 6.259(9)(7)\text{GeV}. \tag{15}$$

Here the first error comes from the fit and the second error from the shifts applied to include missing real world effects as well as experimental uncertainties in the η_b and η_c masses. As can be seen, this is a sizeable part of the total error in this case. We also include in this second error an estimate of sea quark mass effects using results from [10]. There we saw no such for an equivalent quantity for m_{D_s} within 1 MeV statistical errors and so take that as the error here. Table VIII gives the complete error budget for $\Delta_{B_c,bb}$ breaking down both errors into their components.

Our result for M_{B_c} can be compared to experiment (6.277(6) GeV) and to our result from lattice QCD using a completely different formalism, NRQCD, for the b

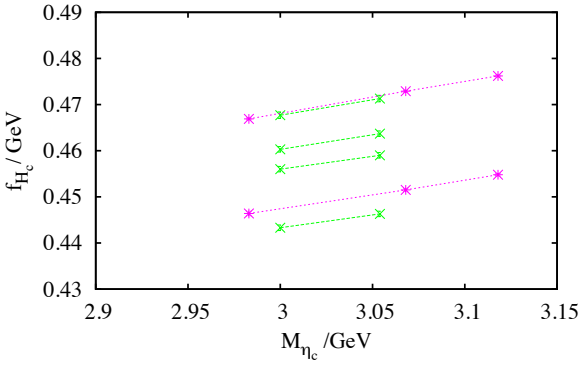

FIG. 6: Results for the heavy-charm decay constant plotted as a function of the c quark mass, given by the mass of the η_c meson. Results are given for multiple heavy quark masses on fine lattices (pink bursts) and superfine lattices (green crosses). Lines are drawn to guide the eye.

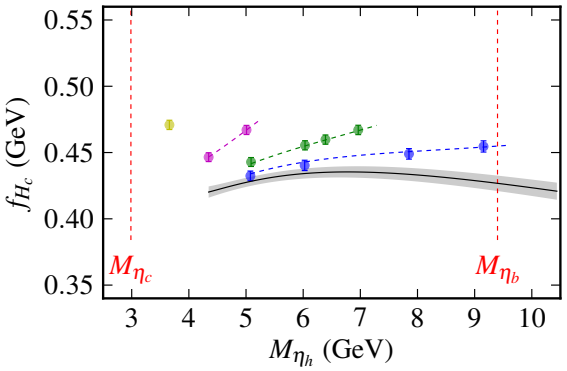

FIG. 7: Results for the heavy-charm decay constant plotted as a function of the pseudoscalar heavyonium mass. Results for coarse, fine, superfine and ultrafine lattices appear from left to right. The lattice QCD results have been adjusted for slight mistuning of the c quark mass. The colored dashed lines give the fitted function for that lattice spacing. The black line with grey error band gives the physical curve derived from our fit.

quark (6.280(10) GeV [18]). We agree, within 2σ with both results even allowing for the fact that the comparison within lattice QCD can be done before any shifts are made or errors allowed for them. This is a strong confirmation of the control over errors that we now have in lattice QCD.

The method given here for determining m_{B_c} (as for the method for m_{B_s} in section III B) does depend on the experimental η_b mass; the mass difference determined in lattice QCD is not particularly sensitive to it but when the mass is reconstructed from the difference, $m_{\eta_b}/2$ is added in. Recent results from the Belle collaboration [29] have $M_{\eta_b} = 9.402(2)$ GeV, significantly higher than the previous world-average [17]. Using the Belle result for M_{η_b} pushes our values for m_{B_c} and m_{B_s} 6 MeV higher. In both cases this improves the agreement with experiment but is not significant given the 11 MeV error. Note that our earlier NRQCD results are hardly affected at all by a change in the η_b mass because they determined a mass difference to the spin-average of the Υ and η_b masses, which is dominated by the Υ mass.

Results for the H_c decay constant, f_{H_c}, are also given in Table VII. The rate for B_c leptonic decay to $l\nu$ via a W boson is proportional to the square of the decay constant multiplied by CKM element V_{cb} as in eq. (4). In practice this decay will be very hard to see experimentally, but a lattice QCD calculation of the decay constant also provides a useful test for phenomenological model calculations.

The results at different values of m_c can again be used to tune the decay constant accurately to the result at the physical c quark mass. Figure 6 shows the dependence of f_{H_c} on M_{η_c} acting as a proxy for the c quark mass. Results on fine and superfine lattices are shown – there is clear agreement on the physical slope of f_{H_c} with M_{η_c} between superfine and fine and it does not vary with the heavy quark mass. The slope is small, approximately 0.06, but clearly visible. We will compare this to the slope for f_{H_s} with m_s in section IV.

The H_c decay constant is plotted as a function of M_{η_h} in Figure 7. Notice that it is much flatter than the corresponding plot for f_{η_h} (Figure 1). We expect behaviour as $1/\sqrt{M_{\eta_h}}$ whether we view heavy-charm as a heavy-light system (in which case the behaviour will be similar to heavy-strange) or as a heavy-heavy system (in which case the argument becomes that $\psi(0)$ depends on the reduced mass μ, tending to m_c for large m_h, and then the decay constant falls as the square root of the heavy mass).

As before, we fit f_{H_c} to the function of M_{η_h} (above 4 GeV) described in section II. We take the leading term given in Table III to be that expected from HQET arguments appropriate to heavy-light physics. Our fit has $\chi^2 = 0.7$ for 11 degrees of freedom and gives result:

$$f_{B_c} = 0.427(6)(2)\text{GeV}. \tag{16}$$

Here the first error is from the fit and the second from additional systematic effects missing from our lattice QCD calculation. These we estimate based on the arguments given for the η_h in section III A. The error from missing electromagnetism and from sea quark mass effects we take to be the same as for the η_b at 0.4% and 0.1% respectively; missing c in the sea should be a factor of m_c/m_b smaller at 0.04%. Table VIII gives the complete error budget.

f_{B_c} can be converted into a branching fraction for leptonic decay using the formula of eq. (4) and the unitarity value of V_{cb}. We predict a branching fraction to $\tau\nu$ of 0.0194(18). The error here comes mainly from the experimental determination of the B_c lifetime with a smaller effect from the uncertainty in V_{cb}. Our value for f_{B_c} contributes a 3% error. Because of helicity suppression the

branching fraction smaller for other lepton final states (8×10^{-5} to $\mu\nu$, for example).

The value we obtain for f_{B_c} can be compared to results from potential models. As discussed earlier in the context of f_{η_h}, potential model results have a lot of variability and raw values for $\psi(0)$ need renormalisation. A more useful comparison is to compare ratios. Our lattice QCD results give $f_{B_c}/f_{\eta_c} = 1.08(1)$ and $f_{\eta_h}/f_{B_c} = 1.57(2)$. The range of potentials considered in [22] give values from 0.90 to 1.02 for f_{B_c}/f_{η_c} and 1.34 to 1.72 for f_{η_h}/f_{B_c}. Again the largest number is always from the Cornell potential. Potential model values for $\psi(0)$ converted to f_{B_c} simply using $f = \psi(0)\sqrt{12/M_{B_c}}$ yield results varying from 0.5 to 0.7 GeV i.e. significantly larger than the well-defined value for f_{B_c} from lattice QCD.

The values for f_{B_c} from potential models provide input to estimates of the production cross-section of the B_c at the LHC. In the factorisation approach the cross-section is proportional to the square of f_{B_c}, with typical values for f_{B_c} being taken as 0.48 GeV [30]. Our results indicate that this could be leading to a 25% overestimate of the production rate.

IV. DISCUSSION

An interesting issue is to what extent the B_c meson is a heavy-heavy particle and to what extent, a heavy-light one at the physical values we have for b and c quark masses. Here we address this by comparing the behaviour of B_c properties to those of η_h and B_s using the results from section III.

An alternative to calculating $\Delta_{H_c,hh}$ to study the heavy-charm meson mass is to take differences between heavy-charm and heavy-strange and charm-strange mesons. We define

$$\Delta_{H_c,hs} = M_{H_s} + M_{D_s} - M_{H_c}, \tag{17}$$

so that $\Delta_{H_c,hs}$ is a positive quantity. Once again it amounts to a difference in binding energies but now between a set of mesons that are all effectively 'heavy-light' states. Indeed a study of $\Delta_{H_c,hs}$ shows us to what extent the B_c can be considered a heavy-light particle rather than, or as well as, a heavy-heavy one.

Figure 8 shows $\Delta_{H_c,hs}$, with all results tuned accurately to the correct c and s masses, as a function of the heavy quark mass, again given by the η_h mass. In fact $\Delta_{H_c,hs}$ shows very little dependence on the heavy quark mass above a value of M_{η_h} of about 6 GeV. HQET would expect the leading m_h-dependent piece of $\Delta_{B_c,hs}$ to be given by the difference of the expectation values of the kinetic energy operator, $p_h^2/2m_h$, for the heavy quark in a heavy-charm meson and a heavy-strange meson, ignoring the effect of spin-dependent terms which are expected to be smaller. Figure 8 shows that this difference is not large i.e. the charm quark is behaving in a similar way to a light quark (but does have a larger expectation value for its kinetic energy operator as might be expected) when combined with a heavy quark of order twice its mass or heavier.

We fit $m_{H_c,hs}$ as described in section II and using the fit form and priors tabulated in Table III. Our fit has χ^2 of 0.3 for 14 degrees of freedom. It returns the coefficient of the first term in $M_{\eta_h}^{-1}$ as $-0.4(8)\text{GeV}/M_{\eta_h}$. This quantifies the statement made above about the slope of $1/m_h$ corrections. The coefficient is not very accurately determined because we allow for many higher order terms. In fact the sign of the slope is clear from Figure 8 with a positive slope with M_{η_h} corresponding to a negative value for the coefficient of the $1/M$ term, as expected.

The variation of $\Delta_{H_c,hs}$ with M_{η_c} agrees well with that found in our calculation using NRQCD b quarks [18] giving a slope of 0.07 at the b. Likewise the variation with $M_{\eta_s}^2$ also agrees well with the slope of 0.4 found in [18].

Our fit to $\Delta H_c, hs$ is independent of our earlier fit to $\Delta_{H_c,hh}$ (although it uses some of the same numbers) and so the results provide a consistency check. We find at $h = b$ that:

$$\Delta_{B_c,bs} = 1.052(9)(3)\text{GeV} \tag{18}$$

which agrees well within 1σ with the same quantity calculated using NRQCD b quarks [18]. The result when $h = c$ is consistent within 1σ with double the result from $m_{D_s} - m_{\eta_c}/2$ given in [10]. The first error above is from the fit and the second from the systematic error for sea quark mass effects, taking the same 1 MeV as for $\Delta_{B_c,bb}$, and the effects of missing electromagnetism and c in the sea. The shifts and errors for these latter effects are given in Table II and we take those errors to be correlated. The value above for $\Delta_{B_c,bs}$ combined with experimental results for M_{B_s} and M_{D_s} [17] (the net shift from Table II amounts to a negligible 0.2 MeV) gives:

$$M_{B_c} = 6.285(9)(3)\text{GeV}, \tag{19}$$

consistent within 2σ with our result from $\Delta_{B_c,bb}$ given in section III, and slightly more accurate. We therefore adopt it as our final result here. The complete error budget for $\Delta_{B_s,bs}$ is given in Table VIII.

In figure 9 we show the ratio of η_h and H_c decay constants to that of the H_s, plotted from our physical curves as a function of M_{η_h}. The ratio f_{η_h}/f_{H_s} rises strongly with M_{η_h}, because of the big difference in the dynamics of heavy-heavy and heavy-strange mesons, whereas the ratio f_{H_c}/f_{H_s} tends to a constant at large M_{η_h}. As explained in section III C this latter behaviour would be expected whether the heavy-charm is viewed as a heavy-heavy or heavy-light state, because the reduced mass of the heavy-charm system is controlled by the charm mass in the large heavy mass limit.

Further insight comes from comparing the dependence of the heavy-charm and heavy-strange decay constants on m_c and m_s respectively. Figure 10 plots the relative change of f_{H_c} or f_{H_s} to its value at the tuned mass point for a given relative change in the light quark mass. The strange quark mass is monitored by the value of $M_{\eta_s}^2$,

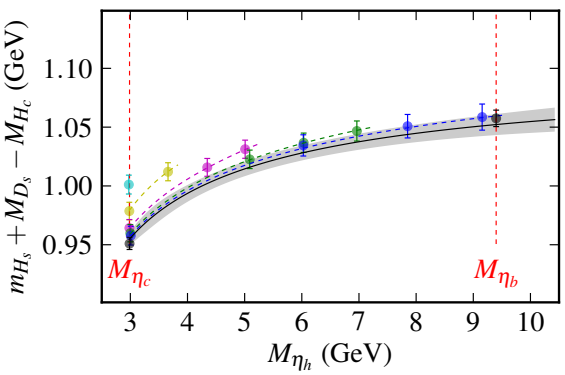

FIG. 8: Results for the mass difference between the heavy-charm meson and the corresponding heavy-strange and charm-strange mesons plotted as a function of the pseudoscalar heavyonium mass. Results for coarse, fine, superfine and ultrafine lattices appear from left to right. The lattice QCD results have been adjusted for slight mistuning of the c and s quark masses. The colored dashed lines give the fitted function for that lattice spacing. The black line with grey error band gives the physical curve derived from our fit. The black circles with error bars at M_{η_b} and M_{η_c} give experimental values adjusted for the effects from electromagnetism, η_b/η_c annihilation and c quarks in the sea, none of which is included in the lattice QCD calculation.

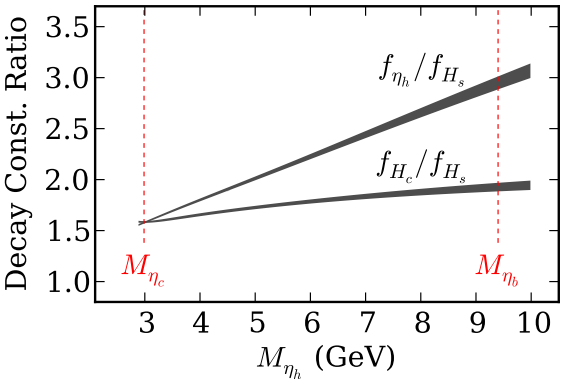

FIG. 9: Results for the ratio of pseudoscalar decay constants, heavy-charm and heavy-heavy to heavy-strange plotted as a function of the pseudoscalar heavyonium mass. The results are obtained from the physical curves given in Figures 1, 3 and 7.

the charm mass by M_{η_c}. The results come from the fine lattices, set 3, where we have multiple m_c and m_s values close to the tuned point. Results are plotted for two values of the heavy quark mass, $m_h a = 0.7$ and $m_h a = 0.85$ but little difference between them is seen.

The dependence of f_{H_s} on m_s is not very strong [4], as expected since f_{H_s} and f_H differ only by around 20% for a change by a factor of 27 in light quark mass. The dependence of f_{H_c} on m_c is larger by about a factor of

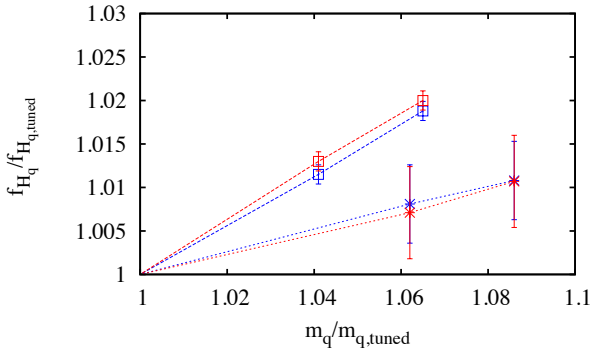

FIG. 10: Comparison of the effect of 'detuning' the charm and strange quark masses on the heavy-charm and heavy-strange decay constants. Open squares show the fractional change in f_{H_c} for a given fractional change in M_{η_c} (as proxy for m_c) for two different heavy quark masses (in blue $m_h a = 0.7$ and red $m_h a = 0.85$) on the fine lattices set 3. Burst show the fractional change in f_{H_s} for a given fractional change in $M^2_{\eta_s}$ (as proxy for m_s) for the same two heavy quark masses on set 3. Lines are drawn to guide the eye.

M_{η_h}	f_{η_h}	f_{H_s}	f_{H_c}	$\Delta_{H_s,hh}$	$\Delta_{H_c,hh}$	$\Delta_{H_c,hs}$
3	0.394(2)	0.249(2)	–	0.477(2)	0.000(0)	0.956(6)
4	0.452(2)	0.251(2)	0.417(6)	0.520(3)	0.004(1)	0.994(7)
5	0.501(3)	0.249(2)	0.427(3)	0.554(4)	0.015(1)	1.014(6)
6	0.546(4)	0.244(3)	0.434(4)	0.581(6)	0.027(2)	1.028(6)
7	0.586(4)	0.237(3)	0.435(4)	0.605(7)	0.039(3)	1.038(7)
8	0.623(5)	0.231(4)	0.433(5)	0.626(9)	0.050(5)	1.045(8)
9	0.655(6)	0.224(4)	0.429(6)	0.645(11)	0.061(8)	1.050(8)

TABLE IX: Values for the various quantities that we fit here evaluated at masses, M_{η_h}, between that of c and b. These are obtained from our fit functions at $a = 0$ and tuned s and c masses. All numbers are in GeV. There is no result for f_{H_c} at 3 GeV because that point is not included in that fit.

two. However the slope of the Figure 10 is 1/3 (see also Figure 6), much less than the slope of 1 expected if $f_{B_c} \propto m_c$. This latter behaviour would be approximately that expected in a heavy-heavy picture in which $\psi(0) \propto \mu$, with the reduced mass, μ, close to m_c in the B_c case. The linear behaviour of $\psi(0)$ would be consistent with the picture we have of the η_h in Figure 1, where $\mu \approx M_{\eta_h}/4$, using $b \approx 0.5$.

V. CONCLUSIONS

By using a relativistic approach to heavy quarks (HISQ) which has relatively small discretisation errors we have been able to map out the dependence on heavy quark mass of the pseudoscalar heavyonium, heavy-strange and heavy-charm decay constants and the heavy-strange and heavy-charm meson masses, complementing results in [3, 4].

We find the heavyonium decay constant surprisingly

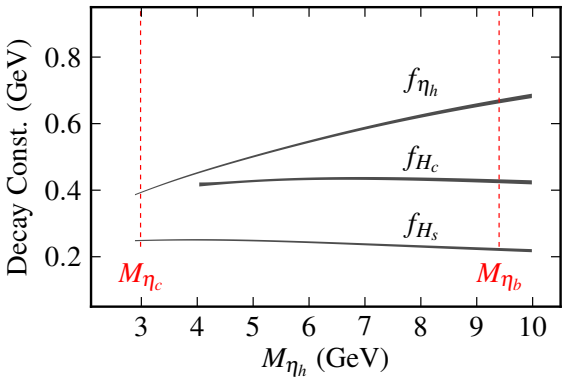

FIG. 11: Summary of heavy quark mass dependence of decay constants for the pseudoscalar H_c, H_s and η_h mesons. The grey bands show our physical curves from Figures 1, 3 and 7.

close in value to the experimental results for the charmonium and bottomonium vector decay constants. Work is underway to confirm this result using NRQCD for the heavy quark and to establish accurate results for the corresponding vector decay constants in lattice QCD. Although the η_h decay constant has no simple connection to an observed experimental rate, it is useful for comparison and calibration of lattice QCD calculations in heavy quark physics since it can be determined to 1%, as we have done here.

Our result for the B_c meson mass agrees well using the two different mass splittings, $\Delta_{B_c,hh}$ and $\Delta_{B_c,hs}$ and also agrees with the experimental value. This is confirmation of our earlier result [18] using NRQCD b quarks and HISQ light quarks.

We determine the B_c decay constant as 427(6) MeV, for the first time in full QCD, predicting a leptonic branching ratio for the B_c to $\tau\nu$ of 1.9(2)% (where the uncertainty comes from t_{B_c}, not f_{B_c}). Our result for f_{B_c} is significantly smaller than that from some potential model calculations, including those being used to estimate LHC production cross-sections [30]. The best way to determine the B_c leptonic decay rate, and hence f_{B_c}, from experiment may be using a high luminosity e^+e^- collider operating at the Z peak [36, 37].

By mapping out the dependence on the heavy quark mass of the H_c, H_s and η_h decay constants we are able to see the differences between the three systems. This is summarised in Figure 11 where we give the physical curves determined from our fits. In section IV we provide evidence that the B_c behaves, at least in some ways, more like a heavy-light system than a heavy-heavy one. We previously noticed this effect in [38] when finding that the mass difference between B_c^* and B_c was very close to the difference between B_s^* and B_s.

Table IX gives results extracted from our fits at intermediate values of M_{η_h} from M_{η_c} to M_{η_b} for comparison to future lattice QCD calculations or to phenomenological models. The values are determined by evaluating our fit function in the continuum limit and at tuned s and c masses, corresponding to the black line in Figs. 1, 2, 3, 4, 7 and 8.

In Figure 12 we summarise the current picture for the decay constants of gold-plated mesons, determined from lattice QCD and from experiment. For lattice QCD we use the best existing results which dominate the world averages [1, 4, 10, 11, 31, 32]. For the experimental values for the unflavored vectors we use leptonic widths to e^+e^- from the Particle Data Tables [17] and eq. (10). For the flavored pseudoscalars the determination of the decay constant from experiment requires the input of a value for the associated CKM element, for example from the unitarity fit to the CKM matrix [17]. We update the D and D_s experimental determinations to the averages including new results from BESIII [34] and Belle [35] respectively.

This plot goes beyond the traditional plot of the mass spectrum [1] to look at a number which is related to the internal structure of the meson. The energy scale for decay constants is controlled by internal momenta inside the meson and so is much compressed over the scale for masses (which covers a large range simply because quark masses have a large range). The pseudoscalar meson decay constants are well filled in but more work is needed to obtain the vector decay constants to the same level of accuracy. This is underway and once complete, this plot will provide a very stringent test of QCD that would be impossible with any method other than lattice QCD.

From our results here and in [3, 4] we see that the relativistic heavy quark approach using the HISQ formalism can successfully give results for the b quark. Future work will use even finer lattices. For $a = 0.03$fm, for example, the b quark mass in lattice units is around 0.5 and so we can easily achieve this mass without the need for extrapolation.

Acknowledgements We are grateful to the MILC collaboration for the use of their configurations and to C. Parkes for useful discussions. Computing was done at the Ohio Supercomputer Center, the Argonne Leadership Computing Facility at Argonne National Laboratory, supported by the Office of Science of the U.S. Department of Energy under Contract DOE-AC02-06CH11357 and facilities of the DEISA consortium (www.deisa.eu) through the DEISA Extreme Computing Initiative, co-funded through the EU FP6 project RI-031513 and FP7 project RI-222919. We acknowledge the use of Chroma [39] for part of our analysis. Funding for this work came from MICINN (grants FPA2009-09638 and FPA2008-10732 and the Ramon y Cajal program), DGIID-DGA (grant 2007-E24/2), the EU (ITN-STRONGnet, PITN-GA-2009-238353), the NSF, the Royal Society, the Wolfson Foundation, the Scottish Universities Physics Alliance and STFC.

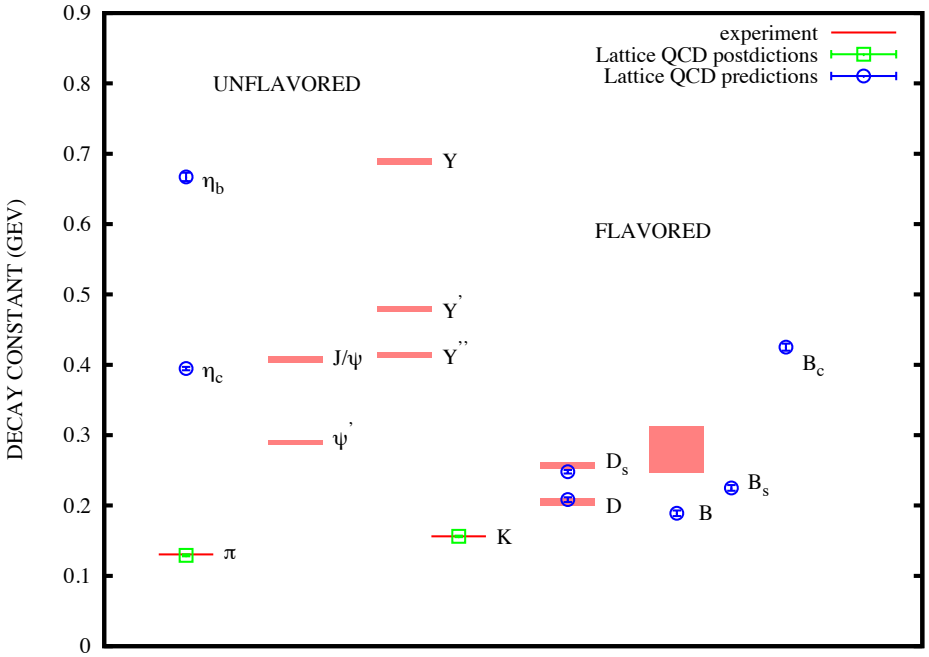

FIG. 12: Spectrum of the decay constants of gold-plated particles from experiment (using values for CKM elements where needed) and from lattice QCD. Lattice QCD results are divided into postdictions (green open squares) and predictions (blue open circles). Results for f_{B_c} and f_{η_b} come from this paper, f_{D_s} and f_{η_c} from [10], f_π and f_K from [31], f_B from [11] and f_D from [32]. Experimental results are given by red shaded bars. For unflavored vector mesons these come from [17] using eq. (10). f_π and f_K are from [17, 33], f_D is the updated experimental average from [34] and f_{D_s}, from [35]. f_B is not well-determined from experiment. We use the result from [1] using averages from [17].

[1] C. Davies, PoS **LATTICE2011**, 019 (2011), 1203.3862.
[2] C. Davies et al. (HPQCD, UKQCD, MILC and Fermilab Lattice Collaborations), Phys.Rev.Lett. **92**, 022001 (2004), hep-lat/0304004.
[3] C. McNeile, C. Davies, E. Follana, K. Hornbostel, and G. Lepage (HPQCD Collaboration), Phys.Rev. **D82**, 034512 (2010), 1004.4285.
[4] C. McNeile, C. Davies, E. Follana, K. Hornbostel, and G. Lepage (HPQCD Collaboration), Phys.Rev. **D85**, 031503 (2012), 1110.4510.
[5] E. Follana et al. (HPQCD Collaboration), Phys.Rev. **D75**, 054502 (2007), hep-lat/0610092.
[6] E. Follana, C. Davies, G. Lepage, and J. Shigemitsu (HPQCD Collaboration), Phys.Rev.Lett. **100**, 062002 (2008), 0706.1726.
[7] R. Dowdall et al. (HPQCD Collaboration), Phys.Rev. **D85**, 054509 (2012), 1110.6887.
[8] A. X. El-Khadra, A. S. Kronfeld, and P. B. Mackenzie, Phys.Rev. **D55**, 3933 (1997), hep-lat/9604004.
[9] G. P. Lepage, L. Magnea, C. Nakhleh, U. Magnea, and K. Hornbostel, Phys.Rev. **D46**, 4052 (1992), hep-lat/9205007.
[10] C. Davies, C. McNeile, E. Follana, G. Lepage, H. Na, et al. (HPQCD Collaboration), Phys.Rev. **D82**, 114504 (2010), 1008.4018.
[11] H. Na, C. J. Monahan, C. T. Davies, R. Horgan, G. P. Lepage, et al. (HPQCD Collaboration) (2012), 1202.4914.
[12] J. Koponen et al. (HPQCD Collaboration), PoS **LATTICE2010**, 231 (2010), 1011.1208.
[13] A. Bazavov, D. Toussaint, C. Bernard, J. Laiho, C. DeTar, et al., Rev.Mod.Phys. **82**, 1349 (2010), 0903.3598.
[14] C. Davies, E. Follana, I. Kendall, G. P. Lepage, and C. McNeile (HPQCD Collaboration), Phys.Rev. **D81**, 034506 (2010), 0910.1229.
[15] G. P. Lepage et al., Nucl. Phys. Proc. Suppl. **106**, 12 (2002), hep-lat/0110175.
[16] A. J. Buras, pp. 281–539 (1998), hep-ph/9806471.
[17] K. Nakamura et al. (Particle Data Group), J. Phys. **G37**, 075021 (2010).
[18] E. B. Gregory, C. T. Davies, I. D. Kendall, J. Koponen, K. Wong, et al. (HPQCD Collaboration), Phys.Rev. **D83**, 014506 (2011), 1010.3848.
[19] M. Neubert, Phys.Rept. **245**, 259 (1994), hep-ph/9306320.
[20] C. Davies et al. (HPQCD Collaboration), Phys.Rev. **D78**, 114507 (2008), 0807.1687.
[21] W. Kwong, J. L. Rosner, and C. Quigg, Ann.Rev.Nucl.Part.Sci. **37**, 325 (1987).
[22] E. J. Eichten and C. Quigg, Phys.Rev. **D52**, 1726 (1995), hep-ph/9503356.
[23] F. Close, AN INTRODUCTION TO QUARKS AND PARTONS **Academic Press** (1979).
[24] J. Erler, Phys.Rev. **D59**, 054008 (1999), hep-

ph/9803453.
[25] A. Gray, I. Allison, C. Davies, E. Dalgic, G. Lepage, et al. (HPQCD Collaboration), Phys.Rev. **D72**, 094507 (2005), hep-lat/0507013.
[26] T. Aaltonen et al. (CDF Collaboration), Phys.Rev.Lett. **100**, 182002 (2008), 0712.1506.
[27] V. Abazov et al. (D0 Collaboration), Phys.Rev.Lett. **101**, 012001 (2008), 0802.4258.
[28] I. F. Allison, C. T. H. Davies, A. Gray, A. S. Kronfeld, P. B. Mackenzie, and J. N. Simone (HPQCD and Fermilab Lattice collaborations), Phys. Rev. Lett. **94**, 172001 (2005), hep-lat/0411027.
[29] R. Mizuk et al. (Belle Collaboration) (2012), 1205.6351.
[30] C.-H. Chang, C.-F. Qiao, J.-X. Wang, and X.-G. Wu, Phys.Rev. **D72**, 114009 (2005), hep-ph/0509040.
[31] A. Bazavov et al. (MILC Collaboration), PoS **LATTICE2010**, 074 (2010), 1012.0868.
[32] H. Na, C. T. Davies, E. Follana, G. P. Lepage, and J. Shigemitsu (2012), 1206.4936.
[33] J. L. Rosner and S. Stone (2012), 1201.2401.
[34] G. Rong (BESIII Collaboration), talk at Charm2012 (2012).
[35] A. Zupanc (Belle Collaboration), talk at Charm2012 (2012).
[36] A. Akeroyd, C. H. Chen, and S. Recksiegel, Phys.Rev. **D77**, 115018 (2008), 0803.3517.
[37] Z. Yang, X.-G. Wu, G. Chen, Q.-L. Liao, and J.-W. Zhang, Phys.Rev. **D85**, 094015 (2012), 1112.5169.
[38] E. Gregory, C. Davies, E. Follana, E. Gamiz, I. Kendall, et al. (HPQCD Collaboration), Phys.Rev.Lett. **104**, 022001 (2010), 0909.4462.
[39] R. G. Edwards and B. Joo (SciDAC, LHPC and UKQCD Collaborations), Nucl.Phys.Proc.Suppl. **140**, 832 (2005), hep-lat/0409003.